

High-symmetry high-stability silicon fullerenes: A first-principles study

Aristides D. Zdetsis

Department of Physics, University of Patras, GR-26500 Patras, Greece

(Received 10 May 2007; published 3 August 2007)

It is shown by *ab initio* calculations that very stable high-symmetry fullerenes of the form Si_nH_n , $n=20, 28, 30, 36, 50,$ and 60 , can be formed with large energy gaps suitable for optoelectronic and other applications. Quantum confinement seems to be violated if one neglects the essentially two-dimensional nature of the electron gas. Comparison with similar carbon fullerenes, such as $\text{C}_{20}\text{H}_{20}$ and $\text{C}_{60}\text{H}_{60}$, reveals full similarity in their electronic and geometrical structures, which is suggestive of possible routes for their synthesis. These silicon fullerenes constitute the best manifestation of carbon and silicon homology.

DOI: 10.1103/PhysRevB.76.075402

PACS number(s): 61.46.Hk, 31.90.+s, 81.05.Tp

Carbon and silicon are both in the fourth column of the Periodic Table, sharing several similarities in their electronic structure and yet their chemistries are very different. Carbon is essential for life, while silicon is essential for modern electronic technology. Carbon normally forms strong π bonds through sp^2 hybridization, which can facilitate two-dimensional spherical cages (or planar structures such as benzene). Silicon, on the other hand, usually forms covalent σ bonds through sp^3 hybridization, which favor three-dimensional diamondlike structures. Thus the structural chemistries of carbon and silicon are different and yet similar. Almost immediately after the discovery and synthesis¹ of C_{60} , great expectations for the synthesis of similar silicon fullerenes were generated. This includes not only Si_{60} in analogy to C_{60} but also smaller fullerenes such as C_{20} . The synthesis of C_{20} , which is the smallest carbon fullerene, by high voltage dehydrogenation² of $\text{C}_{20}\text{H}_{20}$ is considered as the most dramatic experiment reported to date.³ The synthesis of $\text{C}_{20}\text{H}_{20}$ itself was a difficult challenge and was first achieved by Paquette *et al.*,⁴ and later by Prinzbach *et al.*⁵ using improved routes.

Up to now, the most successful approach for the formation of small relatively stable silicon fullerenes is the endohedral doping of some silicon cage-like clusters with a suitable transition metal atom.^{6–8} However, this approach is limited to very small sizes of cages, normally in the region of 10–20 silicon atoms. For full-fledged transition metal atoms with unfilled d electronic shells, the bonding is dominated by the filling of empty d shells of the transition metal atom by silicon-cage electrons.⁸ The role of the transition metal atom, as has been illustrated by the present author,⁸ is similar to the saturation of the silicon dangling bonds of the “cage” by hydrogen. Therefore, the obvious extension of this analogy is to attempt to replace their assumed roles. With this initial thought in mind, an extensive and exhaustive search for Si_nH_n , $n \leq 60$, fullerenes was initiated. Kumar and Kawazoe^{7(b)} in their study of hydrogen interaction with $M@Si_m$ metal ($M=\text{Cr}, \text{Mo}, \text{W},$ and Zr) embedded silicon cages, $m=12, 16,$ and 18 , have also considered (in a different context) empty hydrogenated silicon cage-like clusters Si_mH_m , with $m=12, 16,$ and 20 .

The general method of calculation for all fullerenes was the density functional theory (DFT) within the hybrid, non-local exchange and correlation functional of Becke-Lee, Parr, and Yang.⁹ The calculations were performed with the TURBO-

MOL program package¹⁰ using the TZVP basis sets.¹¹ The accuracy of this method, in particular, for silicon and hydrogenated silicon nanoclusters, has been tested before by comparison to high level *ab initio* methods (such as the multireference second order perturbation theory).^{8,12} For smaller fullerenes (up to $n=24$), second order many body perturbation theory was also used for comparison (for both geometry optimization and total energy calculations). Extensive and exhaustive (at least for the smaller fullerenes with $n \leq 30$) stability tests (including random distortions of various sizes and systematic distortions toward “bulky” hydrogenated nanocrystals such as those of Ref. 12) have been performed together with vibrational analysis in order to test and verify the (global) static and dynamical stabilities of these fullerenes. The most stringent tests have been performed for nanocrystals with $n=20, 24,$ and 28 . For these cages, stability tests besides distortions include transformations to more condensed systems involving hydrogen and/or silicon loss or gain. At the same time, analogous reverse transformations were performed on “nearby” bulky nanocrystals such as $\text{Si}_{17}\text{H}_{36}$ and $\text{Si}_{29}\text{H}_{36}$.¹² No better minima could be found. These additional tests verified the standard stability tests (on top of vibrational analysis) performed for all “small” cages (up to $n=30$). Vibrational analysis and limited distortions against bulky systems were performed for all cages up to $n=60$. Thus, all “fullerenes” are proven local minima (with real vibrational frequencies) and have very large highest occupied molecular orbital (HOMO) lowest unoccupied molecular orbital (LUMO) gaps. Nevertheless, for such large systems, there is no guarantee (especially for the larger clusters) that the structures are real global minima.

The most stable structures found are shown in Figs. 1(a) and 1(b). All these structures have unusually high symmetries (icosahedral, tetrahedral, etc., without Jahn-Teller distortions), real frequencies, and large HOMO-LUMO gaps, as shown in Table I. As in the case of carbon fullerenes, the “turning point” occurs at $n=20$. The structures with $n < 20$ are considerably less stable (with binding energies smaller than 6.20 eV/atom) and not always the lowest possible energetically.^{7(b),8} For instance, for $n=12$, another “bulky cage” of D_{2d} symmetry (see Fig. 8 of Ref. 8) is lower in energy than the D_{6h} structure⁸ of Fig. 1(a). This type of structures in the work of Kumar and Kawazoe^{7(b)} appear to have larger binding energies and smaller HOMO-LUMO gaps. The structures with $n \geq 20$, contrary to the $n < 20$ structures,

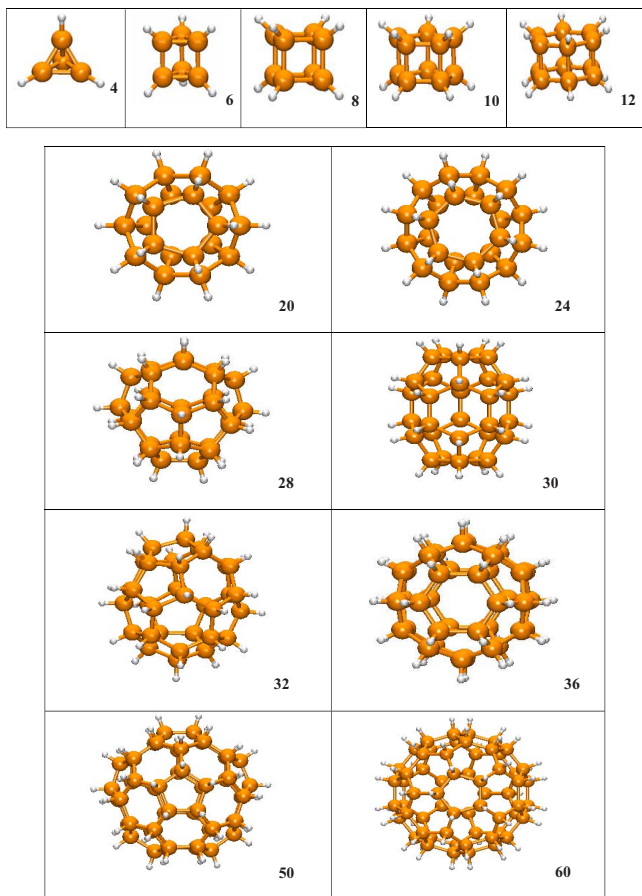


FIG. 1. (Color online) The high-symmetry high-stability structures of Si_nH_n , $n=4, \dots, 60$ cages.

are fully analogous (structurally and electronically) to the corresponding C_nH_n fullerenes.

In particular, for the $\text{Si}_{20}\text{H}_{20}$ cluster which is, indeed, the turning point, the geometrical and electronic structures

TABLE I. Binding energies per Si-H pair (E_b), HOMO-LUMO energy gaps (H-L), and symmetry group (Sym.) of the cages.

n	E_b (eV/atom)	H-L (eV)	Sym.
4	5.057	4.089	T_d
6	5.690	4.387	D_{3h}
8	5.965	4.230	O_h
10	6.100	4.492	D_{5h}
12	6.100	4.145	D_{6h}
20	6.356	4.367	I_h
24	6.350	4.259	D_{6d}
28	6.348	4.380	T_d
30	6.348	4.443	D_{5h}
32	6.340	4.371	D_{3d}
36	6.334	4.432	D_{6h}
50	6.308	4.587	D_{5h}
60	6.291	4.665	I_h

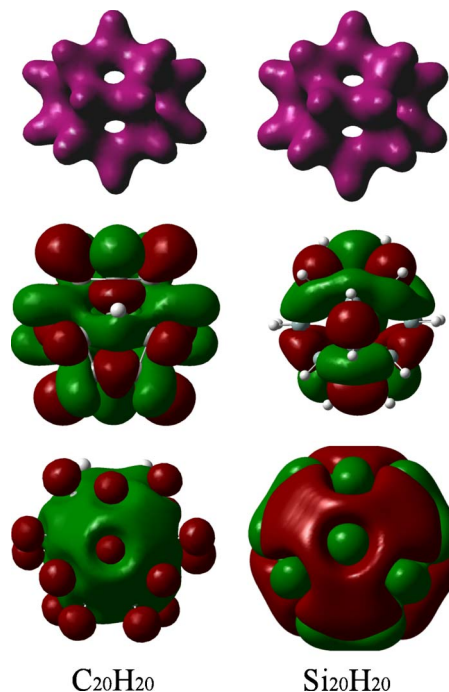


FIG. 2. (Color online) Charge density (top), HOMO (in the middle), and LUMO (bottom) orbitals of $\text{C}_{20}\text{H}_{20}$ (left) and $\text{Si}_{20}\text{H}_{20}$ (right) fullerenes.

(charge density, HOMO and LUMO orbitals), as shown in Fig. 2, are fully analogous to the corresponding $\text{C}_{20}\text{H}_{20}$ (dodecahedrane).

Dodecahedrane is a fascinating molecule with unusually high symmetry, the synthesis of which (a difficult but tractable problem^{4,5}) eventually led also to the synthesis of the smallest carbon fullerene C_{20} . Dodecahedrane ($\text{C}_{20}\text{H}_{20}$) has been studied at various levels of theory with regard to electronic, chemical, and thermochemical properties.

In particular, the energies and stabilities of the endohedral $X@C_{20}H_{20}$ and exohedral $XC_{20}H_{20}$ complexes have been extensively studied^{3,13} for a large number of host atoms and ions X (where $X=\text{H}^+$, H, He, $\text{Li}^{0/+}$, $\text{Be}^{0/+2+}$, Ne, Ar, N, P, C^- , Si^- , O^+ , S^+ , $\text{Na}^{0/+}$, and $\text{Mg}^{0/+2+}$) for various chemical and technical applications. In addition, atomic hydrogen encapsulated in deuterated $\text{C}_{20}\text{D}_{20}$ has been proposed for use as single quantum bits (qubits) in solid state quantum computers.¹⁴

Therefore it could be expected that $\text{Si}_{20}\text{H}_{20}$ would have similar multiple applications. Its synthesis could be “analogous” to the synthesis of $\text{C}_{20}\text{H}_{20}$ since their bonding and structural properties appear to be homologous. However, further reduction to icosahedral Si_{20} through high voltage dehydrogenation or other analogous technique seems to be unlikely in view of the destabilizing dangling bonds, which for carbon are not a problem due to sp^2 bonding. Thus, Si_{20} and C_{20} are not homologous. It becomes clear, therefore, that the closest we can get to silicon fullerenes analogous to carbon fullerenes is by synthesizing the corresponding hydrogenated cages (perhaps with methods analogous to the corresponding carbon fullerenes, although this might seem highly improbable in view of the complicated organic chemical reactions

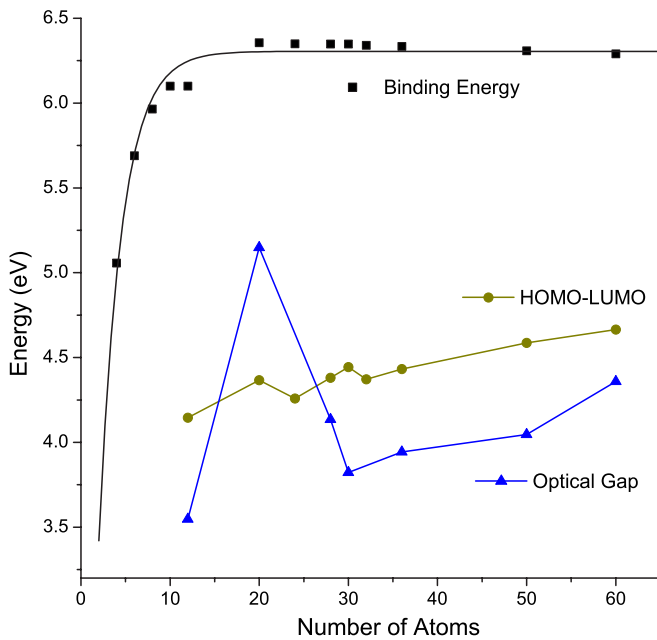


FIG. 3. (Color online) Binding energy per silicon atom and HOMO-LUMO and optical gaps as a function of silicon (or hydrogen) atoms.

involved for the corresponding carbon cages). This is true for most of the fullerenes in Fig. 1(b). For instance, the $\text{Si}_{60}\text{H}_{60}$ fullerene is “homologous” to $\text{C}_{60}\text{H}_{60}$, which was reported to have been discovered in stellar atmospheres,¹⁵ although it has not been synthesized in the laboratory up to now. Here, too, endohedral complexes such as H_2 , CO , and LiH have been examined¹⁶ and found more stable than the corresponding complexes with C_{60} . Similar results would be expected, therefore, for $\text{Si}_{60}\text{H}_{60}$ and most of the fullerenes in Table I (with $n \geq 20$).

Looking closer at Table I, we can see that $\text{Si}_{20}\text{H}_{20}$ has the highest binding energy and (therefore) stability, although all fullerenes above $n=20$ have also high binding energies (well above 6.20 eV/atom) and well above the binding energies of the cages with n below 20. The binding energy versus the number of silicon (or hydrogen) atoms n together with the HOMO-LUMO and optical gaps is shown in Fig. 3. The binding energy is a very slowly (monotonically) decreasing function of n . Since the average Si-Si and Si-H distances remain practically constant, this small decrease in binding energy must be mainly related to an increase in hydrogen-hydrogen (proton-proton) repulsion. Indeed, adjacent hydrogen atoms come closer as the size of the cage increases and its curvature decreases. For instance, the H-H distance in $\text{Si}_{20}\text{H}_{20}$ is 3.42 Å compared to 2.98 Å in $\text{Si}_{60}\text{H}_{60}$ (for $\text{Si}_{28}\text{H}_{28}$, the H-H distance has an intermediate value of 3.18 Å). The corresponding Si-H bond has practically the same length in both cages, although the Si-Si bond length is decreased slightly from 2.37 Å in $\text{Si}_{20}\text{H}_{20}$ to 2.34 Å in $\text{Si}_{60}\text{H}_{60}$.

Another characteristic of Table I and Fig. 3 that is remarkable is the variation of the HOMO-LUMO gap with the size of the fullerene, determined by the number of Si-H pairs n . As we can see in the table, with the exception of some small

fluctuations, the size of the gap increases with increasing cage size. This seems to contradict the idea of quantum confinement (see, for instance, Ref. 12), which demands larger gaps for smaller sizes. However, a closer look reveals that this is not so due to the two-dimensional (2D) nature of the cages. Because of the spherical (on the average) shape of the cages, as the radius increases, the number of atoms (in the surface) increases roughly proportionally to the square of the radius, but due to the 2D nature of the cages (all atoms at the surface) the effective volume increases also proportionally to the square of the radius. As a result, we would expect that the average volume per atom (and per electron) should remain practically constant (at least, for very large cages). However, these proportionalities (due to the distinct distribution and finite size of the cages) are not exact. Actually, as we saw earlier, the Si-Si bond lengths of $\text{Si}_{60}\text{H}_{60}$ compared to those of $\text{Si}_{20}\text{H}_{20}$ have been reduced by about 1.3%. We can estimate the effective volume per electron $V_{\text{eff}}^{(e)}$, by drawing two concentric spheres with radii R_{H} and R_{Si} (or $\langle R_{\text{H}} \rangle$ and $\langle R_{\text{Si}} \rangle$ for nonspherical cages) up to the layer of hydrogen and silicon, respectively.

If N_e is the number of electrons,

$$V_{\text{eff}}^{(e)} = \frac{1}{N_e} \frac{4\pi}{3} (\langle R_{\text{H}} \rangle^3 - \langle R_{\text{Si}} \rangle^3),$$

we find $V_{\text{eff}}^{(e)}[\text{Si}_{20}\text{H}_{20}] = 1.04 \text{ \AA}^3/\text{electron}$ and $V_{\text{eff}}^{(e)}[\text{Si}_{60}\text{H}_{60}] = 0.91 \text{ \AA}^3/\text{electron}$. Therefore, “confinement” is stronger in the case of $\text{Si}_{60}\text{H}_{60}$ and, as a consequence, the gap is larger in $\text{Si}_{60}\text{H}_{60}$. As an additional test, we calculate $V_{\text{eff}}^{(e)}$ for $\text{Si}_{12}\text{H}_{12}$ for which the HOMO-LUMO gap is smaller compared to $\text{Si}_{20}\text{H}_{20}$. In this case, we find $V_{\text{eff}}^{(e)}[\text{Si}_{12}\text{H}_{12}] = 1.24 \text{ \AA}^3/\text{electron}$, in agreement with “quantum confinement.” It could be argued that the quantum confinement concept is not fully applicable to saturated systems such as the Si_nH_n cages. Nevertheless, almost all of the theoretical models used to describe quantum confinement (successfully) in porous silicon and silicon nanocrystals use fully saturated silicon atoms at the surface.¹²

The optical gap in Fig. 3, calculated with the time dependent DFT method, is defined as the energy of the first allowed (by symmetry) excitation. There are several strange but important features in the variation of the optical gap versus the number of atoms as follows:

(1) The irregularity of the curve illustrates that the optical absorption gaps and spectral properties of these fullerenes are size, shape, and symmetry dependent (and apparently composition dependent after endohedral or exohedral doping). Therefore the optical properties of these fullerenes can be tuned broadly in the ultraviolet-visible region. This is very important for optoelectronic applications.

(2) Comparing the optical gap variation versus number of atoms in Fig. 3 with similar curves for hydrogenated silicon nanocrystals of comparable sizes¹² [see, for instance, Table II and Fig. 1 in Ref. 12(a)], which show smooth monotonic variation of the gap, reveals the sharp dependence of the gap on the symmetry of the fullerenes. Apparently, the HOMO-LUMO gap is less sensitive to symmetry. It should be noted

that all nanocrystals in Ref. 12 share the same tetrahedral symmetry and spherical shape.

(3) Similar comparison of the HOMO-LUMO in relation to the optical gap for the present fullerenes and the bulky hydrogenated nanocrystals in Ref. 12 shows markedly different behaviors. Whereas for the hydrogenated nanocrystals the HOMO-LUMO gap is always larger than the optical gap (the difference giving the quasiparticle relaxation energy), for the hydrogenated cages, this is not always true. The obvious example for this difference is the behavior of $\text{Si}_{20}\text{H}_{20}$. As we can see in Fig. 3, the optical gap of this fullerene is the largest compared to the rest of the fullerenes, and larger than its own HOMO-LUMO gap. This is easy to explain if we look closer at the symmetry of the HOMO and LUMO orbitals and the symmetry of the allowed transitions. The HOMO orbital is characterized by h_u symmetry and the LUMO by a_g . This transition is not allowed by symmetry. Due to the high I_h symmetry of $\text{Si}_{20}\text{H}_{20}$, the only allowed singlet transitions are those of t_{1u} symmetry. The first t_{1u} excitation which determines the optical gap is located at 5.148 eV above the ground state. As a result, the HOMO-LUMO gap cannot be used to estimate the experimental band-gap optical transition. The same effect is also present in several other high-symmetry (icosahedral, dodecahedral, and tetrahedral) molecules and clusters.¹⁷ Symmetry breaking (lowering) is the key to achieving lower (in the visible region of the spectrum) singlet excitations (and optical gaps) and higher dipole moments. Such symmetry lowering can be easily achieved through endohedral or exohedral doping, which, as we have seen already, is very popular and very effective with this material(s) or its carbon counterpart(s). For example, $\text{C}_{20}\text{H}_{20}$ has a completely similar behavior: its HOMO and LUMO orbitals have the same a_g symmetry with a HOMO-LUMO gap of 7.3 eV, whereas the optical gap has been blueshifted by 2.1 eV. For $\text{Si}_{60}\text{H}_{60}$, however, although the HOMO (symmetry h_u) to LUMO (symmetry t_{2u}) excitation is forbidden, the first allowed t_{1u} transition is only 4.36 eV above the ground state compared to the HOMO-LUMO gap of 4.665 eV. In this case, the optical gap is redshifted by about 0.3 eV.

(4) A final point which comes out of Fig. 3 is the relation of the optical gap to quantum confinement. The role of the HOMO-LUMO gap has been already examined and explained above. However, contrary to the hydrogenated silicon nanocrystals for which the two curves are almost parallel and without crossing each other,¹² for the silicon fullerenes the two curves (HOMO-LUMO and optical gaps versus n) do cross and follow a different pattern. To see how this affects quantum confinement, let us concentrate on the two

icosahedral fullerenes $\text{Si}_{20}\text{H}_{20}$ and $\text{Si}_{60}\text{H}_{60}$. Their HOMO-LUMO gap relation was shown to be consistent with quantum confinement on the basis of the average effective volume per electron. This argument explains the variation of the HOMO-LUMO gap of the other fullerenes as well. However, the same argument cannot be used for the optical gaps of $\text{Si}_{20}\text{H}_{20}$ and $\text{Si}_{60}\text{H}_{60}$, since $\text{Si}_{20}\text{H}_{20}$ has a much larger optical gap than $\text{Si}_{60}\text{H}_{60}$. A possible explanation is obtained by considering, instead of the average effective volume per electron, the total effective volume occupied by all electrons of the cage, Ω_{eff} , through which we can define an effective sphere radius r_{eff} . We find $\Omega_{\text{eff}}[\text{Si}_{20}\text{H}_{20}]=312 \text{ \AA}^3$ and $\Omega_{\text{eff}}[\text{Si}_{60}\text{H}_{60}]=819 \text{ \AA}^3$, with $r_{\text{eff}}[\text{Si}_{20}\text{H}_{20}]=4.21 \text{ \AA}$ and $r_{\text{eff}}[\text{Si}_{60}\text{H}_{60}]=5.82 \text{ \AA}$. In this respect, the “electron gas” in $\text{Si}_{60}\text{H}_{60}$ is less confined and, therefore, is characterized by a smaller optical gap compared to $\text{Si}_{20}\text{H}_{20}$. Comparing with the bulky hydrogenated silicon nanocrystals of Ref. 12, we can see that, in this region of radii, the closest nanocrystals are $\text{Si}_{17}\text{H}_{36}$ and $\text{Si}_{29}\text{H}_{36}$, with optical gaps of comparable magnitude (5.03 and 4.53 eV). Thus, it could be argued that whereas the HOMO-LUMO gap is related to the average effective volume per electron, the optical gap pertains to the total effective volume occupied by all electrons of the cage.

In conclusion, it has been demonstrated that silicon fullerenes of the form Si_nH_n with $n \geq 20$ are fascinating stable “molecules” with exceptionally high symmetry and stability and very large HOMO-LUMO and optical gaps. These silicon fullerenes are fully homologous (structurally and electronically) to the corresponding C_nH_n carbon fullerenes, such as $\text{Si}_{20}\text{H}_{20}$, which have been synthesized using various techniques and have been also extensively studied for various chemical (through endohedral and exohedral doping) and optoelectronic applications (tailoring of the optical gap). The above silicon fullerenes, in view of the great similarity to the corresponding carbon fullerenes in structural, bonding, and electronic properties, presumably could be synthesized in “analogous ways” and are expected to have similar chemical and technical applications in electronics, optoelectronics, and quantum computers. It is anticipated that even larger fullerenes with high symmetry and stability also exist, in analogy to the larger known carbon fullerenes. More work is needed in this direction. As a matter of fact, the author only after submission of this manuscript became aware of a recently published work in this direction.¹⁸ Although the context of this work is generally different from the present, the results concerning the relative variation of the stability and HOMO-LUMO gap of $\text{Si}_{20}\text{H}_{20}$ compared to $\text{Si}_{60}\text{H}_{60}$ are in full agreement with the present work.

¹H. W. Kroto *et al.*, Nature (London) **318**, 162 (1985); H. W. Kroto, A. W. Altar, and S. P. Balm, Chem. Rev. (Washington, D.C.) **91**, 1212 (1991).

²H. Prinzbach, A. Weller, P. Landenberger, F. Wahl, J. Worth, L. T. Scott, M. Gelmont, D. Olevano, and B. von Issendorff, Nature (London) **407**, 60 (2000).

³Z. Chen, H. Jiao, D. Moran, A. Hirsch, W. Thiel, and P. v. R. Schleyer, J. Phys. Chem. A **107**, 2075 (2003).

⁴L. A. Paquette, R. J. Temansky, D. W. Balogh, and G. Kentgen, J. Am. Chem. Soc. **105**, 5446 (1983); L. A. Paquette, D. W. Balogh, R. Usha, D. Kountz, and G. G. Christoph, Science **211**, 575 (1981); L. A. Paquette, Chem. Rev. (Washington, D.C.) **89**,

- 1051 (1989).
- ⁵W. D. Fessner *et al.*, *Angew. Chem., Int. Ed. Engl.* **26**, 452 (1987); M. Bertau *et al.*, *Tetrahedron* **53**, 10029 (1997).
- ⁶S. M. Beck, *J. Chem. Phys.* **87**, 4233 (1987); **90**, 6306 (1989).
- ⁷V. Kumar and Y. Kawazoe, *Phys. Rev. Lett.* **87**, 045503 (2001); **90**, 055502 (2003).
- ⁸A. D. Zdetsis, *Phys. Rev. B* **75**, 085409 (2007).
- ⁹P. J. Stephens, F. J. Devlin, C. F. Chabalowski, and M. J. Frisch, *J. Phys. Chem.* **98**, 11623 (1994).
- ¹⁰TURBOMOLE, Version 5.6, Universitat Karlsruhe.
- ¹¹A. Schäfer, C. Huber, and R. Ahlrichs, *J. Chem. Phys.* **100**, 5829 (1994).
- ¹²C. S. Garoufalidis, A. D. Zdetsis, and S. Grimme, *Phys. Rev. Lett.* **87**, 276402 (2001); A. D. Zdetsis, *Rev. Adv. Mater. Sci.* **11**, 56 (2006).
- ¹³D. Moran, F. Stahl, E. D. Jemmis, H. F. Schaefer, and P. v. R. J. Schleyer, *J. Phys. Chem. A* **106**, 5144 (2002).
- ¹⁴S. Park, D. Srivastava, and K. J. Cho, *J. Nanosci. Nanotechnol.* **1**, 1 (2001).
- ¹⁵A. Webster, *Nature (London)* **352**, 412 (1991).
- ¹⁶Y. H. Hu and E. Ruckenstein, *J. Chem. Phys.* **123**, 144303 (2005).
- ¹⁷R. Xie, G. W. Bryant, J. Zhao, T. Kar, and V. H. Smith, Jr., *Phys. Rev. B* **71**, 125422 (2005).
- ¹⁸A. J. Karttunen, M. Linnolahti, and T. A. Pakkanen, *J. Phys. Chem. C* **111**, 2545 (2007).